

# Synthesis and structure determination of copper perrhenate, $\text{CuReO}_4$

D. Mikhailova\*, H. Ehrenberg, H. Fuess

*Institute for Materials Science, Darmstadt University for Technology, Petersenstr. 23, D-64287 Darmstadt, Germany*

Received 23 February 2006; received in revised form 19 March 2006; accepted 26 March 2006

Available online 1 April 2006

## Abstract

Copper(I) perrhenate,  $\text{CuReO}_4$ , has been synthesized as a single-phase sample in sealed silica tubes at 500–800 °C, and its structure was determined for the first time by single-crystal X-ray diffraction.  $\text{CuReO}_4$  forms a new structure type derived from the diamond-structure and crystallizes in space group  $I4_1cd$  with lattice parameters  $a = 13.6965(5) \text{ \AA}$  and  $c = 7.7729(5) \text{ \AA}$ ,  $Z = 16$  (rotation method data acquisition using  $\omega$  and  $\varphi$  scans,  $R_1 = 0.0191$ ,  $wR_2 = 0.0403$ ). Cu and Re atoms are tetrahedrally coordinated by O atoms, these tetrahedra are corner-shared, forming spirally twisted rings of 4-6-8-10- $\text{MeO}_4$  like  $\text{Si}_x\text{O}_y$ -rings in some silicon dioxide modifications or aluminosilicates. According to low-temperature powder X-ray diffraction and differential thermal analysis,  $\text{CuReO}_4$  shows no phase transition down to 80 K and up to its melting point, 703 K.

© 2006 Elsevier Inc. All rights reserved.

**Keywords:** Copper(I) perrhenate;  $\text{CuReO}_4$ ; Tetrahedra network; Acentric structure

## 1. Introduction

Up to now ternary oxides of all  $3d$  elements with Re are known [1–9]. The oxides with  $\text{Re}^{7+}$ , the perrhenates, are easily prepared and therefore the most frequently investigated compounds. They are usually synthesized from aqueous solutions and are stable in air as hydrates. The crystal structures of all  $3d$  metal perrhenates except Ti and Cr have been determined [1–4]. Ternary oxides with low valence Re ( $< +7$ ) are usually prepared under extreme conditions (high-pressure high-temperature synthesis) [6–9]; the detailed crystal structure and magnetic properties are determined only for  $\text{CoReO}_4$  [7],  $\text{MnReO}_4$  [8], and  $\text{V}_{0.5}\text{Re}_{0.5}\text{O}_2$  [9].  $\text{MnReO}_4$  has a monoclinic wolframite-type structure with octahedral coordination of  $\text{Mn}^{2+}$  and  $\text{Re}^{6+}$ . The same structure type was proposed by Sleight [6] for  $\text{ZnReO}_4$ . A compound  $\text{CuReO}_4$  with  $\text{Cu}^{2+}$  is not known, but could also be expected in a wolframite-like structure due to similar  $\text{Cu}^{2+}$  and  $\text{Zn}^{2+}$  ionic radii for coordination number 6 (0.73 and 0.74 Å, respectively [10]).

In the Cu–Re–O-system the copper(II) perrhenate,  $\text{Cu}(\text{ReO}_4)_2$ , has been reported in the literature [5], and

the crystal structure has been solved only for the crystallohydrate  $\text{Cu}(\text{ReO}_4)_2 \cdot 4\text{H}_2\text{O}$  [2]. A few studies were devoted to copper(I) perrhenate,  $\text{CuReO}_4$  [11–13]. It was prepared for the first time as a non-single-phase sample by thermal decomposition of  $\text{Cu}(\text{ReO}_4)_2$  in vacuum [11] at 400–500 °C, its density and melting point have been determined, but neither crystal structure nor cell parameters were examined. Other authors [12] reported the synthesis of  $\text{CuReO}_4$  from Cu and  $\text{Cu}(\text{ReO}_4)_2$  at 360 °C, but no physical–chemical properties have been studied due to the presence of impurities in the sample. In this work [13] the authors used mass-spectrometric methods to measure the composition of the gaseous phase and vapor pressure over the sample containing about 80%  $\text{CuReO}_4$ , prepared from  $\text{Cu}(\text{ReO}_4)_2$  and Cu. It was found that the vapor over  $\text{CuReO}_4$  at 650–780 K consists of  $\text{Re}_2\text{O}_7$  and  $(\text{CuReO}_4)_2$  molecules. The impurity in the  $\text{CuReO}_4$  sample was not identified. Neither crystal structure nor cell parameter were determined. From the literature it is unclear whether the authors of [11–13] have investigated the same compound  $\text{CuReO}_4$ , because two phases with nominal composition  $\text{CuReO}_4$  and different oxidation states of metals (+1 and +7 or +2 and +6) could exist and no diffraction data have been presented. In this work we describe the synthesis of single-phase  $\text{CuReO}_4$

\*Corresponding author. Fax: +49 6151 166023.

E-mail address: [mikhailova@st.tu-darmstadt.de](mailto:mikhailova@st.tu-darmstadt.de) (D. Mikhailova).

(Cu<sup>1+</sup>Re<sup>7+</sup>O<sub>4</sub>), its crystal structure and some physical–chemical properties.

## 2. Experimental

### 2.1. Syntheses

Since no synthesis methods of single-phase CuReO<sub>4</sub> are reported in the literature, different approaches have been tried. Samples of nominal composition CuReO<sub>4</sub> were synthesized in a sealed silica tube using Cu and Re oxides in different oxidation states: CuO (Chempur, 99.99%) and ReO<sub>3</sub> (Strem Chemicals, 99.9%) (I), Cu (Alfa Aesar, 99.99%) and freshly prepared Cu(ReO<sub>4</sub>)<sub>2</sub> (II), Cu<sub>2</sub>O (Alfa Aesar, 99.9%) and Re<sub>2</sub>O<sub>7</sub> (Alfa Aesar, 99.9%) (III). Before use, CuO and ReO<sub>3</sub> were dried in air at 110–120 °C for 2–3 h. The synthesis conditions listed below were tested to achieve the best quality of the samples:

- (I) A stoichiometric mixture of CuO and ReO<sub>3</sub> was ground in an agate mortar under acetone and pressed into pellets, which were placed in a quartz crucible and sealed in an evacuated silica tube.
- (II) Stoichiometric amounts of Cu(ReO<sub>4</sub>)<sub>2</sub> and Cu were weighed in a glove box (< 1 ppm O<sub>2</sub>/H<sub>2</sub>O), mixed and pressed into pellets. Cu(ReO<sub>4</sub>)<sub>2</sub> was prepared from copper(II) basic carbonate (Aldrich) and HReO<sub>4</sub> by a standard method described elsewhere [1]. HReO<sub>4</sub> was obtained from Re powder (Stream, 99.99%) and 30% solution of H<sub>2</sub>O<sub>2</sub> (Aldrich, p.a.). In order to dehydrate pellets of Cu(ReO<sub>4</sub>)<sub>2</sub>·4H<sub>2</sub>O, they were held in dynamic vacuum at 140–160 °C during 2–3 h until the increase of temperature by 10° did not influence the residual pressure. Pellets of the mixture of Cu(ReO<sub>4</sub>)<sub>2</sub> and Cu in a quartz crucible were placed into a silica tube, which was evacuated and sealed.
- (III) A powder mixture of Cu<sub>2</sub>O and Re<sub>2</sub>O<sub>7</sub> oxides in the molar ratio 1:1 was placed within a glove box into a silica tube using a quartz crucible. The tube was sealed under vacuum.

In all cases the reactants were heated at 500–800 °C for 20–30 h.

### 2.2. Single-crystal X-ray diffraction

The crystal structure of CuReO<sub>4</sub> was solved by single-crystal X-ray diffraction using the Xcalibur system from Oxford Diffraction. The software packages SHELXS [14] and SHELXL [15] were used for structure solution and refinement as included in X-STEP32 [16]. A combined empirical absorption correction with frame scaling was applied, using the SCALE3 ABSPACK command in CrysAlisRed [17].

### 2.3. X-ray powder diffraction (XPD) at room temperature and 80 K

Phase analysis and determination of cell parameters were carried out using XPD with a STOE STADI P diffractometer (MoK $\alpha$ <sub>1</sub>-radiation,  $\lambda = 0.7093$  Å) in steps of 0.02° for 2 $\theta$  from 3° to 45° in transmission mode for flat samples or in Debye–Scherrer mode for sealed glass capillaries. All diffraction patterns have been analyzed by full-profile Rietveld refinements, using the software package WinPLOTR [18]. An Oxford Cryosystems Cryostream Cooler (600 Series) with nitrogen gas low temperature attachment was used for the cooling of a ground powder sample in sealed glass capillary of 0.3 mm diameter down to 80 K and stabilized for the collection of X-ray data.

### 2.4. EDX analysis

The cation composition was verified by EDX analysis, performed on different crystallites, using a Philips XL30 FEG microscope.

### 2.5. Differential thermal analysis (DTA-TG)

A simultaneous thermal analyzer NETZSCH STA 429 (CD) operated with dry and purified Ar was used to register mass loss and thermal flux curves. About 70 mg of CuReO<sub>4</sub> were heated in a Pt–Ir-crucible with a rate of 10 °C/min from 20 up to 1070 °C.

### 2.6. Infrared spectroscopy (IRS)

The infrared absorption spectrum of CuReO<sub>4</sub> was obtained on a PERKIN ELMER FTIR 1750-spectrometer. Samples were pressed into pellets, diluted with KBr. Pellets of pure KBr were used as negative control.

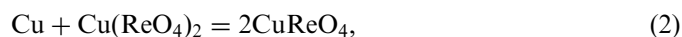
### 2.7. Magnetic susceptibility

The magnetic properties of CuReO<sub>4</sub> have been studied with a superconducting quantum interference device (SQUID) from quantum design. Measurements were performed in the temperature range from 1.8 to 250 K and field strength 50 and 500 Oe.

## 3. Results and discussion

### 3.1. Synthesis and characterization of CuReO<sub>4</sub> samples

The CuReO<sub>4</sub> samples were synthesized in the interval of temperature 500–800 °C by three methods according to reactions:



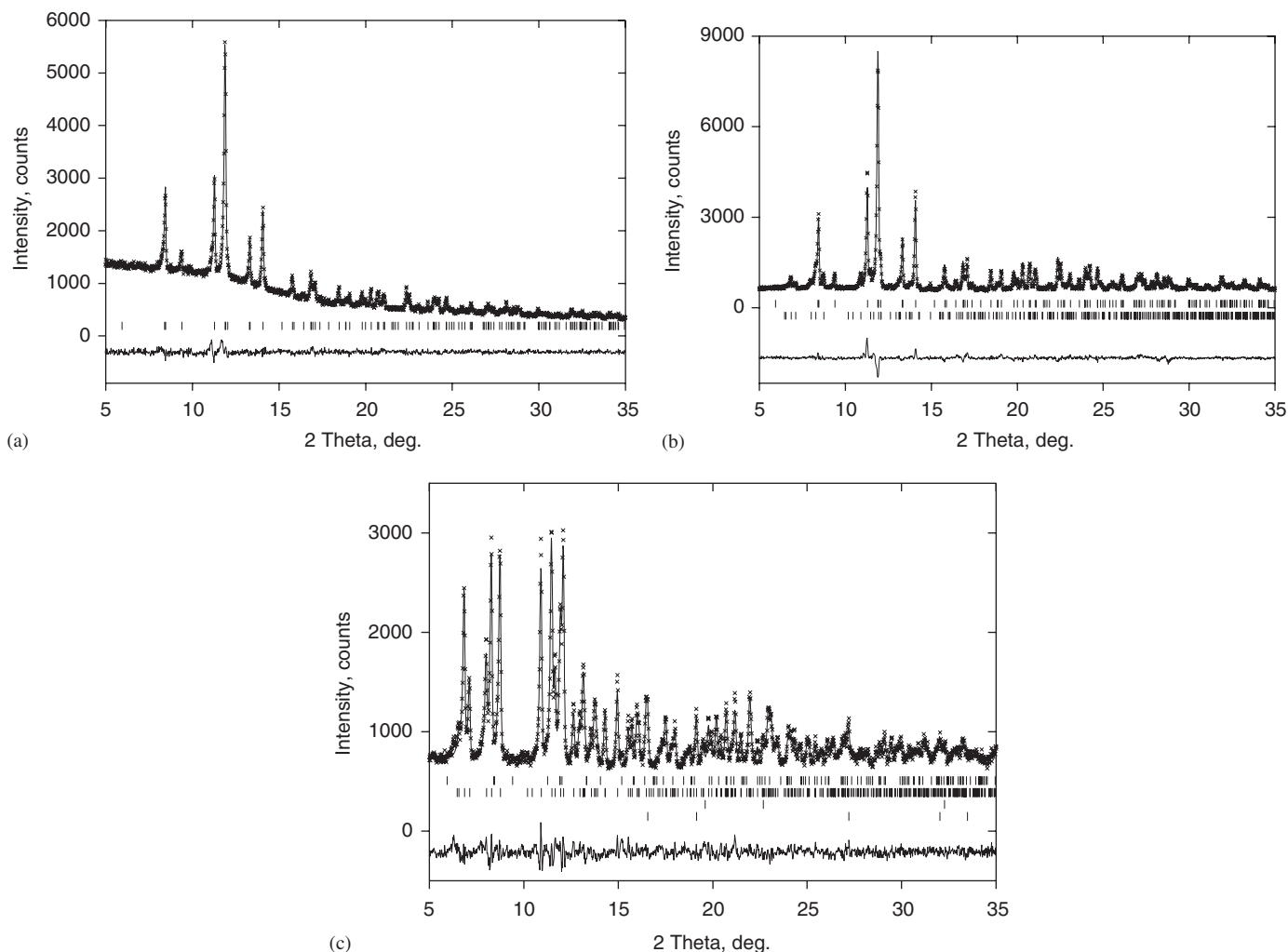
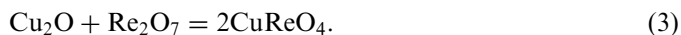


Fig. 1. The observed and fitted profiles for  $\text{CuReO}_4$ , together with the corresponding difference curve ( $\text{Mo-K}\alpha_1$ ). (a) The sample was measured in a capillary, (b) the sample was measured during 3 hours in air, (c) the sample was left one month in air before measuring, the fitted profiles belong to the phases  $\text{CuReO}_4$ ,  $\text{Cu}(\text{ReO}_4)_2 \cdot 4\text{H}_2\text{O}$ ,  $\text{Cu}$  and  $\text{Cu}_2\text{O}$  (from top to bottom, respectively).

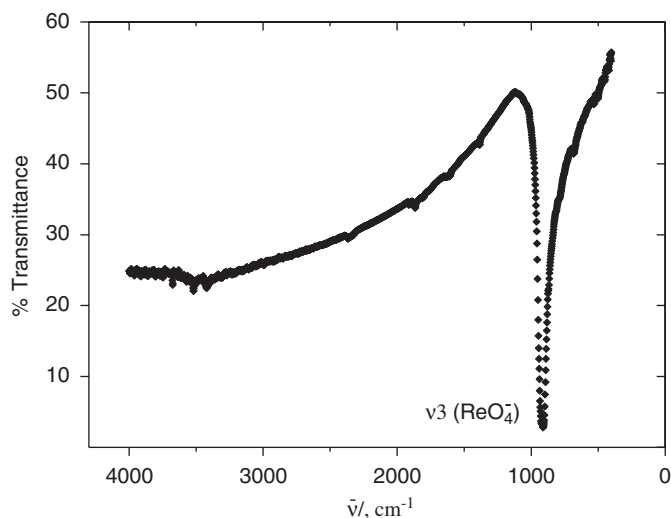
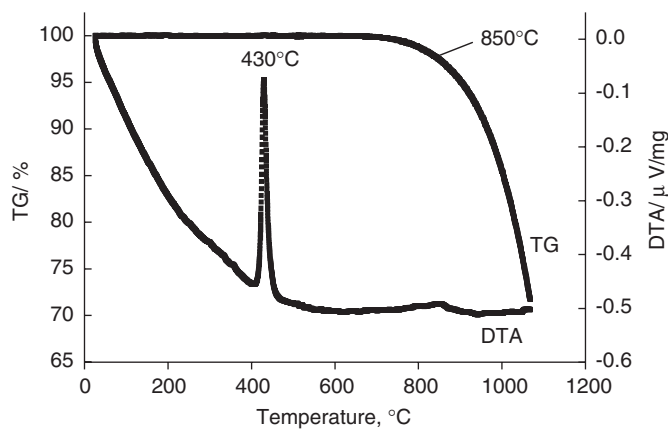


They appeared as dark-brown cakes, which indicated the occurrence of melting during syntheses. The breaking of these cakes yielded orange-red crystals. All samples gave similar XPD patterns, and all reflections were explained based on a tetragonal unit cell with lattice parameters  $a = 13.69 \text{ \AA}$  and  $c = 7.77 \text{ \AA}$ . Fig. 1(a) shows the diffraction pattern of the sample prepared by reaction (3).

The  $\text{Re}_2\text{O}_7$  partial pressure over  $\text{CuReO}_4$  calculated from the equation  $\lg p(\text{Re}_2\text{O}_7, \text{Pa}) = -9561/T + 11.82$  [13], is  $8 \times 10^{-3} \text{ atm}$  at  $800^\circ\text{C}$ , corresponding to  $\sim 6 \times 10^{-7} \text{ mol Re}_2\text{O}_7$  or 0.1 wt% Re of the overall Re mass in the reaction tube. At  $500^\circ\text{C}$  it is  $\sim 0.00005 \text{ wt\% Re}$ . The EDX analysis of some thin  $\text{CuReO}_4$  fragments of the sample, prepared at  $800^\circ\text{C}$ , indicated that the average metal ratio Cu:Re is 1:1, in agreement with nominal composition (data not shown). The compound appears to be diamagnetic, because no distinct magnetic signal from  $\text{CuReO}_4$  was registered at SQUID at field strengths 50 and 500 Oe.

The reaction with water was used to proof the oxidation states of Cu and Re, since the precipitate of a compound, containing  $\text{Cu}^{2+}$  and  $\text{Re}^{6+}$  would consist of  $\text{ReO}_2$ , because all compounds with  $\text{Re}^{6+}$  disproportionate in aqueous solution in  $\text{ReO}_4^-$  and  $\text{ReO}_2$ . On the other hand, Cu is expected to precipitate in the solution of a  $\text{Cu}^{1+}$  containing compound [19].  $\text{CuReO}_4$  decomposes in water immediately forming a precipitate of  $\text{Cu}_2\text{O}$  and  $\text{Cu}$ , according to the X-ray diffraction, and  $\text{Cu}(\text{ReO}_4)_2$  in solution. Therefore, the oxidation states  $\text{Cu}^{1+}/\text{Re}^{7+}$  were assigned in agreement with no detectable paramagnetic moment.

Note that  $\text{CuReO}_4$  is unstable to oxygen and moisture, and 15–20 wt% of  $\text{Cu}(\text{ReO}_4)_2$  as impurity were present in XPD patterns of samples, which have been measured in air during 2–3 h (Fig. 1(b)). A sample of  $\text{CuReO}_4$  kept one month in air (Fig. 1(c)) contained more than 90%  $\text{Cu}(\text{ReO}_4)_2 \cdot 4\text{H}_2\text{O}$ , only 2%  $\text{CuReO}_4$ , 4%  $\text{Cu}_2\text{O}$  and less than 1% Cu. No degradation was observed for a sample, measured in a glass capillary sealed under argon atmosphere (i.e. 100%  $\text{CuReO}_4$ ) (Fig. 1(a)). The behavior of

Fig. 2. The infrared spectrum of CuReO<sub>4</sub>.Fig. 3. TGA data of CuReO<sub>4</sub>.

copper(I) perrhenate in air differs from copper(I) halides CuX ( $X = \text{Cl}, \text{Br}, \text{I}$ ), which are more stable and oxidize according to the reaction  $2\text{CuX} + \text{H}_2\text{O} + 1/2\text{O}_2 = 2\text{Cu}(\text{OH})\text{X}$  [19].

The IR-spectrum of CuReO<sub>4</sub> in the interval of 4000–500  $\text{cm}^{-1}$  contains only one peak at  $\sim 920 \text{ cm}^{-1}$  (Fig. 2), which corresponds to the  $\nu_3$ -vibration of the tetrahedral ion  $\text{ReO}_4^-$  [20] (Figs. 2 and 6).

The TGA data of CuReO<sub>4</sub> are presented in Fig. 3. The DTA-curve shows two endothermic peaks, the one at 430 °C is due to the melting of CuReO<sub>4</sub> and the other above 850 °C corresponds to an evaporation of CuReO<sub>4</sub> and in part to the decomposition of the sample to Cu<sub>2</sub>O and Re<sub>2</sub>O<sub>7</sub>(g). The residue after the measurement consisted only of CuReO<sub>4</sub>. This indicates an evaporation of CuReO<sub>4</sub> according to the reaction  $2\text{CuReO}_4(\text{s}) = (\text{CuReO}_4)_2(\text{g})$ , which is known for alkali-metal perrhenates [21]. This result does not confirm previous findings [13], who reported the presence of Re<sub>2</sub>O<sub>7</sub> in significant amount in the gas phase over CuReO<sub>4</sub> according to the reaction

Table 1

Details of X-ray single-crystal data collection and structure refinement of CuReO<sub>4</sub>

Crystal data	
Chemical formula	CuO <sub>4</sub> Re
Formula weight	313.74
Crystal system	Tetragonal
Space group	$I4_1cd$
Unit-cell dimensions	$a = 13.6965(5) \text{ \AA}$ , $c = 7.7729(5) \text{ \AA}$
Cell volume	$1458.15(12) \text{ \AA}^3$
Z	16
Calculated density ( $\text{g/cm}^3$ )	5.716
Temperature	293(2) K
Crystal form, color	Prism, red
Crystal size (mm)	$0.05 \times 0.05 \times 0.18$
Data collection	
Diffractometer	Oxford diffraction Xcalibur (TM); single-crystal X-ray diffractometer with sapphire CCD detector
Data collection method	Rotation method data acquisition using $\omega$ and $\varphi$ scans(s)
Radiation type	MoK $\alpha$ ( $\lambda = 0.71073 \text{ \AA}$ )
No. of reflections for cell parameters	1309
Absorption coefficient	$38.855 \text{ mm}^{-1}$
$F(000)$	2176
$\theta$ range for data collection	$2.97$ to $26.36^\circ$
Range of $h, k, l$	$-16 \leq h \leq 16$ , $-17 \leq k \leq 16$ , $-9 \leq l \leq 9$
Reflections collected/unique	2084/662 [ $R_{\text{int}} = 0.0199$ ]
Completeness to $\theta = 26.36^\circ$	99.3%
Refinement method	
Data/restraints/parameters	662/1/55
Goodness-of-fit on $F^2$	1.104
Final $R$ indices [ $I > 2\sigma(I)$ ]	$R_1 = 0.0180$ , $wR_2 = 0.0400$
$R$ indices (all data)	$R_1 = 0.0191$ , $wR_2 = 0.0403$
Absolute structure parameter	$-0.01(2)$
Largest diff. peak and hole	$1.165$ and $-0.814 \text{ e/\AA}^3$

$2\text{CuReO}_4(\text{s}) = \text{Cu}_2\text{O}(\text{s}) + \text{Re}_2\text{O}_7(\text{g})$ . Our value of the melting point is  $56^\circ$  higher than the value obtained in the work [11]. This may be due to impurities in the sample of [11]. In contrast to Cu(I) halides CuReO<sub>4</sub> has no phase transition before the melting point [22].

### 3.2. Crystal structure of CuReO<sub>4</sub>

A tetragonal unit cell with  $a = 13.6965(5) \text{ \AA}$  and  $c = 7.7729(5) \text{ \AA}$  was determined by X-ray single-crystal structure analysis for the sample synthesized at 800 °C and slowly cooled in the furnace. The structure was solved and refined in space group  $I4_1cd$  (see Table 1). Positional parameters and selected interatomic distances for CuReO<sub>4</sub> are listed in Tables 2 and 3, respectively.

Since no data regarding compounds with analogous parameters were found in the ICSD [23], a new crystal structure type, the CuReO<sub>4</sub>-type is established. Its structure represents a three-dimensional framework formed by tetrahedra of CuO<sub>4</sub> and ReO<sub>4</sub> connected by corner-sharing (Fig. 4). There is a number of large channels with an

Table 2  
Positional and thermal displacement parameters ( $\text{\AA}^2$ ) for  $\text{CuReO}_4$

Atom	Site	$x$	$y$	$z$	Occup.	
Re	16b	0.90191(2)	0.35603(2)	0.25138(11)	1	
Cu	16b	0.1671(1)	0.3809(1)	0.3179(2)	1	
O(1)	16b	0.8756(5)	0.2617(5)	0.3888(9)	1	
O(2)	16b	0.0253(5)	0.3615(5)	0.2151(14)	1	
O(3)	16b	0.8441(6)	0.3373(6)	0.0553(9)	1	
O(4)	16b	0.8610(5)	0.4632(5)	0.3435(12)	1	
Atom	$U_{11}$	$U_{22}$	$U_{33}$	$U_{12}$	$U_{13}$	$U_{23}$
Re	0.0246(2)	0.0199(2)	0.0251(2)	-0.0004(1)	-0.0004(2)	0.0022(2)
Cu	0.0498(8)	0.0529(8)	0.0376(8)	-0.0037(7)	0.0182(7)	0.0034(7)
O(1)	0.057(5)	0.026(3)	0.030(4)	0.004(4)	0.003(4)	0.000(3)
O(2)	0.018(4)	0.069(5)	0.077(7)	-0.002(3)	0.000(4)	-0.009(5)
O(3)	0.048(4)	0.047(4)	0.025(5)	-0.003(4)	-0.005(3)	0.006(3)
O(4)	0.059(5)	0.023(4)	0.063(5)	0.000(3)	0.008(4)	-0.001(4)

Table 3  
Characteristic geometric parameters ( $\text{\AA}$ , deg) for  $\text{CuReO}_4$

Re–O(1)	1.715(7)	O(1)–Re–O(2)	110.0(3)	O(3)–Cu–O(2)	104.3(4)
Re–O(2)	1.715(7)	O(1)–Re–O(4)	108.3(3)	O(1)–Cu–O(4)	100.9(2)
Re–O(3)	1.727(7)	O(2)–Re–O(4)	110.5(3)	O(3)–Cu–O(4)	101.5(3)
Re–O(4)	1.737(7)	O(1)–Re–O(3)	109.9(3)	O(2)–Cu–O(4)	89.7(3)
Cu–O(1)	1.903(7)	O(2)–Re–O(3)	108.2(4)	Re–O(1)–Cu	163.9(4)
Cu–O(2)	2.117(8)	O(4)–Re–O(3)	110.0(4)	Re–O(2)–Cu	147.9(4)
Cu–O(3)	1.945(7)	O(1)–Cu–O(3)	99.5(3)	Re–O(3)–Cu	145.4(4)
Cu–O(4)	2.179(7)	O(1)–Cu–O(2)	151.4(2)	Re–O(4)–Cu	148.5(4)

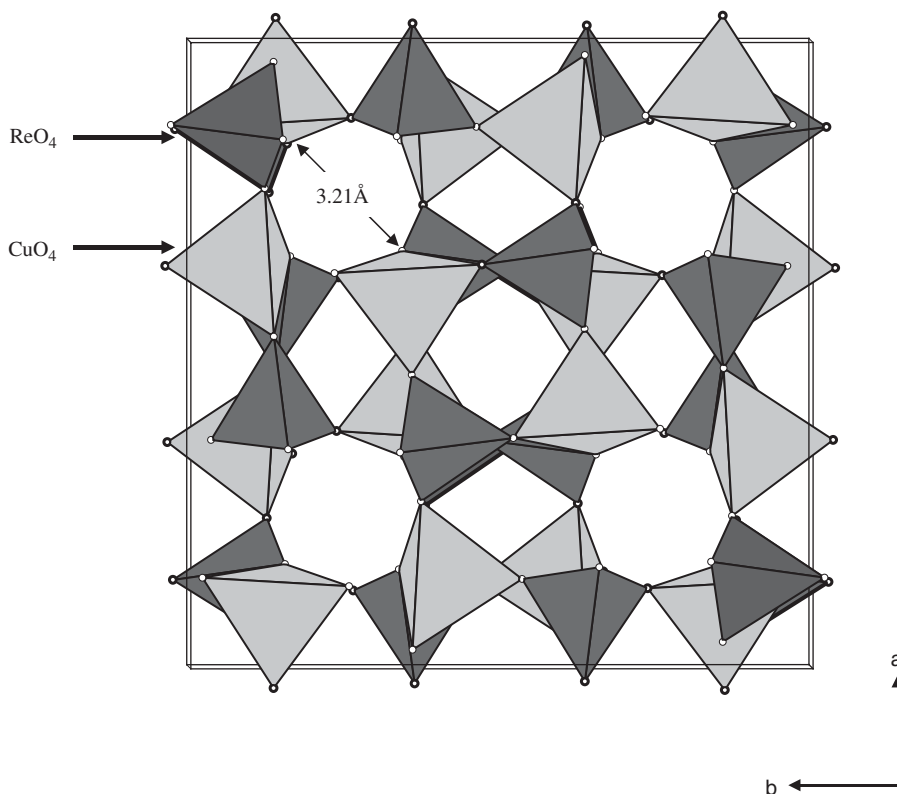


Fig. 4. The crystal structure of  $\text{CuReO}_4$ . Dark gray tetrahedra are occupied by Re atoms, light gray by Cu atoms.



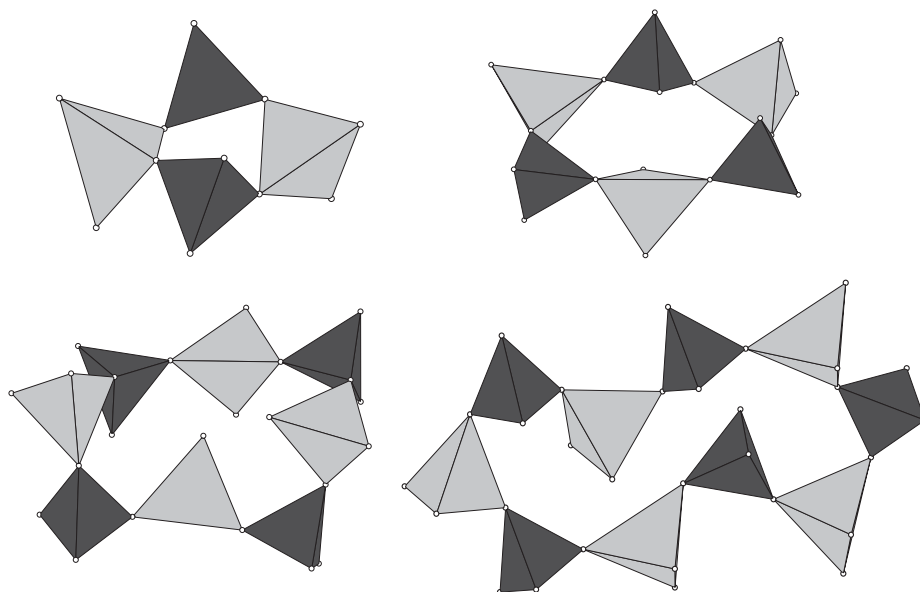


Fig. 5. 4-6-8-10-membered-rings in the framework of  $\text{MO}_4$ -tetrahedra in  $\text{CuReO}_4$ .

average diameter of  $3.1 \text{ \AA}$  between these tetrahedra. It can be suggested that these large channels in the structure facilitate the degradation of  $\text{CuReO}_4$  in air.

The structure of  $\text{CuReO}_4$  can be considered as derived from the diamond-structure and is similar to structures of some silicon dioxides and aluminosilicates [19,24]: the  $\text{CuO}_4$ - and  $\text{ReO}_4$ -tetrahedra form spirally twisted rings of 4-6-8-10- $\text{MeO}_4$ -tetrahedra (Fig. 5) like 6-silica-rings in  $\beta$ -cristobalite or 4-6-8-10-alumo-silica-rings in feldspar  $R^+[\text{AlSi}_3\text{O}_8]$  or  $R^{2+}[\text{Al}_2\text{Si}_2\text{O}_8]$  [24].

All atoms in the structure occupy the same site symmetry (16b); each  $\text{ReO}_4$ -tetrahedron is surrounded by 4  $\text{CuO}_4$ -tetrahedra, and vice versa. This sequence of tetrahedra is subjected to the *Loewenstein-rule*, which has been found for aluminosilicates:  $\text{ReO}_4$ -tetrahedra are never bounded with each other, the structural fragment  $\text{Re-O-Re}$  is avoided [25]. Some interatomic distances and bond angles are listed in Table 3.  $\text{ReO}_4$ -tetrahedra are practically undistorted:  $d_{\text{Re-O}} = 1.715\text{--}1.737 \text{ \AA}$ , the angles  $\text{O-Re-O} = 108.15\text{--}110.54^\circ$ . The average  $\text{Re-O}$  distance ( $d_{\text{Re-O}} = 1.724 \text{ \AA}$ ) is in very good agreement with  $\text{Re-O}$ -distances for  $\text{Re}^{7+}$  located in a tetrahedron of oxygen atoms in  $\text{Re}_2\text{O}_7$  ( $1.70\text{--}1.80 \text{ \AA}$ ) [26], in alkali-metal perrhenates  $M\text{ReO}_4$  ( $M = \text{K}$ ,  $d_{\text{Re-O}} = 1.736 \text{ \AA}$  [27],  $M = \text{Rb}$ ,  $d_{\text{Re-O}} = 1.722 \text{ \AA}$  [28]), in vanadyl perrhenate  $\text{VO}(\text{ReO}_4)_2$  ( $1.69\text{--}1.75 \text{ \AA}$ ) [29] or in  $\text{Cu}(\text{ReO}_4)_2$  ( $1.69\text{--}1.74 \text{ \AA}$ ) [2] (Fig. 6).

The coordination environment of Cu is moderately distorted from ideal tetrahedral symmetry with  $\text{O-Cu-O}$  bond angles (Table 3) ranging from  $90^\circ$  to  $151^\circ$  and bond lengths  $d_{\text{Cu-O}} = 1.903\text{--}2.179 \text{ \AA}$ . The average distance ( $d_{\text{Cu-O}} = 2.036 \text{ \AA}$ ) is significantly larger than  $d_{\text{Cu-O}} = 1.85 \text{ \AA}$  in cuprite  $\text{Cu}_2\text{O}$  (linear oxygen coordination of Cu atoms) and similar to the distance  $\text{Cu-O}$  ( $1.993$  and  $2.031 \text{ \AA}$ ) in  $\text{NaCuO}$  (linear oxygen coordination of Cu atoms, too) [30].

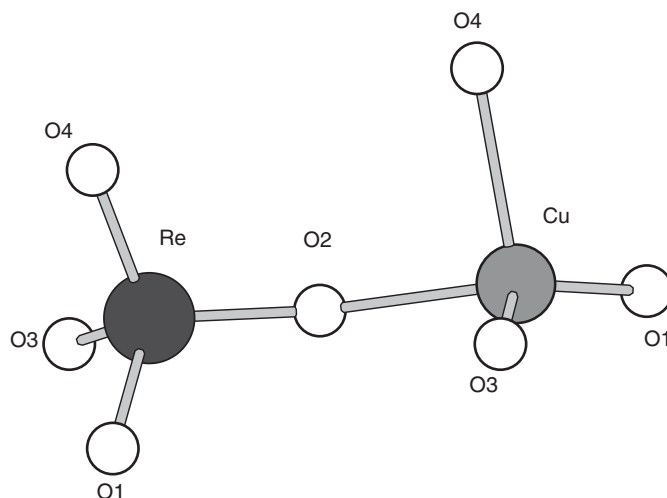


Fig. 6. Oxygen coordination around Cu and Re atoms

A tetrahedral coordination is not unusual for  $\text{Re(VII)}$  and  $\text{Cu(I)}$  cations (for instance,  $\text{CuX}$ , where  $X = \text{Cl}$ ,  $\text{Br}$ ,  $\text{I}$  [19,22]), but there are no examples of  $\text{CuO}_4$  tetrahedra for simple copper(I) compounds [22]. It is interesting to see, how the relative size of cations  $M^+$  in  $M\text{ReO}_4$  influences the structural chemistry of perrhenates of monovalent metals (Table 4). For example, perrhenates of alkali metals ( $M = \text{Na}^+$ ,  $\text{K}^+$ ,  $\text{Rb}^+$ ) and the silver perrhenate  $\text{AgReO}_4$  crystallize in a scheelite-type tetragonal structure, in which  $M$  atoms occupy dodecahedra of O atoms connected by edge-sharing [27,28,31,32]. The thallium(I) and cesium perrhenates,  $\text{TlReO}_4$  [33] and  $\text{CsReO}_4$  [34], crystallize at ambient pressure in a scheelite-like orthorhombic structure with dodecahedral coordination of Tl and Cs.  $\text{LiReO}_4$  and  $\text{CuReO}_4$  are the exception from this row due to their small radii, but they have different structures despite their similar

Table 4  
Ionic radii and crystal structure types of some monovalent perrhenates,  $M\text{ReO}_4$

Ion	Ionic radius for coordination number 6 (Å) [10]	Structural type at room temperature	Coordination polyhedron	Space group	Average M–O bond length (Å)
$\text{Li}^+$	0.76	$\text{LiReO}_4$	Trigonal bipyramid and trigonal pyramid	$P-1$	2.090
$\text{Cu}^+$	0.77	$\text{CuReO}_4$	Tetrahedron	$I4_1cd$	2.065
$\text{Na}^+$	1.02	Scheelite	Dodecahedron	$I4_1/a$	2.025
$\text{Ag}^+$	1.15	Scheelite	Dodecahedron	$I4_1/a$	2.591
$\text{K}^+$	1.38	Scheelite	Dodecahedron	$I4_1/a$	2.802
$\text{Tl}^+$	1.50	Scheelite-like	Dodecahedron	$Pnma$	2.936
$\text{Rb}^+$	1.52	Scheelite	Dodecahedron	$I4_1/a$	2.960
$\text{Cs}^+$	1.67	Scheelite-like	Dodecahedron	$Pnma$	3.184

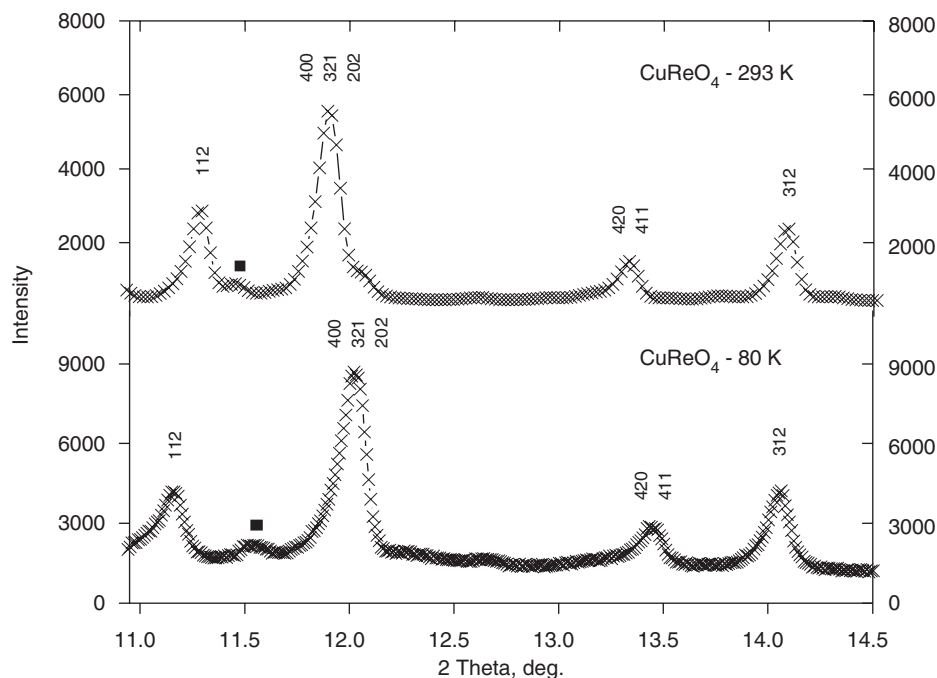


Fig. 7. Selected fragments of the X-ray pattern of  $\text{CuReO}_4$  at different temperatures. The symbol \* indicates the contributions from the impurity  $\text{Cu}(\text{ReO}_4)_2$  formed due to sample handling in air.

sizes:  $\text{Li}^+$  ions occupy in the structure three different crystallographic positions with a distorted trigonal bipyramid and distorted trigonal pyramid from oxygen atoms [35]. Re atoms are tetrahedrally surrounded by O in all these cases. The critical average bond length  $M\text{--O}$  to stabilize the scheelite-type structure seems to be more than 2.5 Å, which corresponds to an ionic radius of more than 1 Å. Note that all these structures except  $\text{CuReO}_4$  are centric structures.

### 3.3. X-ray diffraction of $\text{CuReO}_4$ at low temperature

A sample for X-ray diffraction at 80 K was prepared from CuO and  $\text{ReO}_3$  at 600 °C with quenching after the

synthesis. The diffraction pattern showed no additional peaks in comparison with the pattern at 293 K. In both cases there is a small quantity of  $\text{Cu}(\text{ReO}_4)_2$  in the sample due to sample preparation for analysis in air. Fig. 7 shows two fragments of two diffraction patterns of the same sample  $\text{CuReO}_4$  measured at 293 and 80 K. A distinct peak shift can be seen with decrease of temperature, which indicates a temperature-dependent change of unit cell parameters.

Applying the structure of  $\text{CuReO}_4$  at room temperature as a starting model, a Rietveld refinement of all atomic positions at 80 K was performed with an isotropic approximation for the thermal displacement parameters. The  $z$ -coordinate of Re as the heaviest atom in the structure

was fixed at 0.00. Thermal displacement parameters for all oxygen atoms were fixed at  $1.0 \text{ \AA}^2$  and thermal parameters for the cations were refined separately. After the final refinement good values for the reliability factors were obtained:  $R_p = 2.81\%$ ,  $R_{wp} = 3.60\%$ ,  $\chi^2 = 1.70$ . The parameters “*a*” and “*b*” and the cell volume decrease with decreasing temperature whereas the “*c*” parameter increases:  $a = 13.6812(4) \text{ \AA}$ ,  $c = 7.7615(3) \text{ \AA}$ ,  $V = 1452.76(7) \text{ \AA}^3$  (293K) and  $a = 13.5118(3) \text{ \AA}$ ,  $c = 7.8782(2) \text{ \AA}$ ,  $V = 1438.31(5) \text{ \AA}^3$  (80 K). The average Re–O-distance increases from 1.743 to 1.843 Å, whereas the average Cu–O-distance decreases from 2.025 to 1.969 Å.

Further details of the crystal structure investigation can be obtained from the Fachinformationszentrum Karlsruhe, 76344 Eggenstein-Leopoldshafen, Germany, (fax: +49 7247 808 666; e-mail: crysdata@fiz.karlsruhe.de) on quoting the depository number CSD 416510.

### Acknowledgments

This work was supported by the Deutsche Forschungsgemeinschaft (DFG FU125/42).

### References

- [1] A. Butz, G. Mieke, H. Paulus, P. Strauss, H. Fuess, J. Solid State Chem. 138 (1998) 232.
- [2] M. Varfolomeev, A. Zemenkova, V. Chrustalev, Ju. Struckov, H.-J. Lunk, B. Ziemer, J. Alloy Compd. 215 (1994) 339.
- [3] C. Mujica, K. Peters, E.-M. Peters, H.G. von Schnering, Z. Kristallogr.—New Cryst. St. 213 (1998) 11.
- [4] C. Mujica, K. Peters, E.-M. Peters, W. Carillo, H.G. von Schnering, Bol. Soc. Chil. Quim. 44 (1999) 161.
- [5] L. Zeitseva, et al., Russ. J. Inorg. Chem. 22 (1977) 1185 (Engl. Transl.).
- [6] A.W. Sleight, Inorg. Chem. 14 (1975) 597.
- [7] W.H. Baur, W. Joswig, G. Pieper, D. Kassner, J. Solid State Chem. 99 (1992) 207.
- [8] K.G. Bramnik, H. Ehrenberg, S. Buhre, H. Fuess, Acta Crystallogr. B 61 (2005) 246.
- [9] K.G. Bramnik, H. Ehrenberg, R. Theissmann, H. Fuess, E. Moran, Z. Kristallogr. 218 (2003) 455.
- [10] R.D. Shannon, Acta Crystallogr. A 32 (1976) 751.
- [11] W.T. Smith, J. Am. Chem. Soc. 73 (1951) 77.
- [12] J. Cloarec, A. Deschanvres, B. Raveau, C. R. Acad. Sci. II 264 (1967) 1841.
- [13] K. Skudlarski, W. Lukas, Roczn. Chem. 48 (1974) 745.
- [14] G.M. Sheldrick, Acta Crystallogr. A 46 (1990) 467.
- [15] G.M. Sheldrick, SHELXL97, Program for the Refinement of Crystal Structures, University of Göttingen, Germany, 1997.
- [16] Stoe & Cie, X-STEP32, Stoe & Cie GmbH, Darmstadt, Germany, 2000.
- [17] CrysAlisRed, CCD data reduction GUI, Version 1.171.26, Oxford Diffraction Poland, 2005.
- [18] T. Roisnel, J. Rodriguez-Carvajal, Mater. Sci. Forum 378–381 (2001) 118.
- [19] A.F. Holleman, E. Wiberg, Lehrbuch der Anorganischen Chemie, Walter de Gruyter, Berlin, 1985, p. 1451s.
- [20] K. Nakamoto, Infrared and Raman Spectra of Inorganic and Coordination Compounds, Parts I, II, Wiley, New York, 1997.
- [21] Ye.K. Kazenas, Vaporization Thermodynamics of Double Oxides, Nauka, Moscow, 2004, p. 551s (in Russian).
- [22] A.W. Wells, Structural Inorganic Chemistry, fifth ed., Clarendon Press, Oxford, 1984.
- [23] Inorganic Crystal Structure Database (ICSD), Fachinformationszentrum Karlsruhe, Germany, 2005.
- [24] A. Petzold, W. Hinz, Silikatchemie, Ferdinand Enke Verlag, Stuttgart, 1979, p. 219s.
- [25] W. Loewenstein, Am. Miner. 39 (1954) 92.
- [26] B. Krebs, A. Mueller, H.H. Beyer, Inorg. Chem. 8 (1969) 436.
- [27] J.C. Brown, B.M. Powell, S.N. Stuart, Acta Crystallogr. C 49 (1993) 214.
- [28] P. Roegner, K.-J. Range, Z. Naturforsch. B 48 (1993) 233.
- [29] B. Bastide, R. Enjalbert, H. Fuess, J. Galy, Solid State Sci. 2 (2000) 545.
- [30] R. Hoppe, K. Hestermann, F. Schenk, Z. Anorg. Allg. Chem. 367 (1969) 275.
- [31] A. Atzesdorfer, K.-J. Range, Z. Naturforsch. B 50 (1995) 1417.
- [32] D. Yu. Naumov, A.V. Virovets, S.V. Korenev, A.I. Gubanov, Acta Crystallogr. C 55 (1999) 8.
- [33] A. Jayaraman, G.A. Kourouklis, R.M. Fleming, L.G. Van Uitert, Phys. Rev. B 37 (1) (1988) 664.
- [34] P. Roegner, K.-J. Range, Z. Naturforsch. B 48 (1993) 685.
- [35] T. Betz, R. Hoppe, Z. Anorg. Allg. Chem. 500 (1983) 23.